The Critical Conditions for Tribo-Demagnetization of Perpendicular Magnetic Recording Disk Under Sliding Contact

W. F. Jiang

D. F. Diao[1]
e-mail: dfdiao@mail.xjtu.edu.cn

Key Laboratory of Education Ministry for Modern Design and Rotor-Bearing System,
Xi'an Jiaotong University,
Xi'an 710049, China

The critical conditions (critical stress and critical temperature) for the demagnetization of perpendicular magnetic recording disks were investigated. A tribo-demagnetization test of a perpendicular magnetic recording disk with a low load ball-on-disk system and the scan of the disk with the magnetic head were sequentially carried out to evaluate the critical force and sliding velocity for the occurrence of demagnetization, and the relationship between the two critical factors. Then, a finite element model using thermomechanical coupling was developed to calculate the critical stress and temperature of the magnetic disk based on the critical force and sliding velocity of the experiment result. Finally, a method based on the tribo-demagnetization test in combination with finite element analysis to calculate the critical conditions for the demagnetization of the perpendicular magnetic recording disk under sliding contact was proposed.
[DOI: 10.1115/1.4000734]

Keywords: perpendicular magnetic recording disk, demagnetization, critical conditions, sliding contact, thermalmechanical coupling, finite element analysis

1 Introduction

Perpendicular recording technology has been introduced in hard disk drives (HDDs) for computers because of the high areal recording density and price advantage over longitudinal recording technology in recent years. A typical perpendicular recording medium is made up of various functional layers such as the over coating/lubricant, magnetic recording layer, intermediate layer, soft magnetic underlayer (SUL), and adhesion layer [1]. The soft magnetic underlayer is a significant part of perpendicular recording technology, which makes higher writing fields with single pole head, and smaller grains can be used in the recording medium to achieve higher recording density [2].

Higher areal recording density needs to reduce the over coating thickness on the surface of the magnetic disk and flying height of the head. The head-media spacing has to be reduced to less than 6 nm when the areal recording density of the disk is 1 $Tb/in.^2$ [3]. However, the slider to disk spacing is decreased with the increasing of areal density, which makes the drives more susceptible to several reliability issues, including those head/disk contacts that occur inevitably during the loading and unloading processes at high horizontal velocities or reset by accident, and the probability of contact between the slider and asperities increases. All these contacts probably could generate temperature and stress distributions, as well as mechanical scratching, which could result in permanent loss of data [4,5]. Reduction in the read-back signal amplitude after multiple load/unload cycles was observed by Fu and Bogy [6]. Suk and Gillis [7] studied that the scratches during load/unload processes can induce defects and showed that Hertzian contact stress decreases significantly as a function of the radius of curvature of the slider, and considered the demagnetization for the magnetic disk due to impact stress that resulted from sliding velocity between heads/disks [8]. Nevertheless, data loss has also been observed without any obvious signs of physical damage to the media. Roy and Brand's [9] recent studies showed that frictional heating associated with contact force between the particle and the disk could lead to permanent loss of data. Therefore, knowing the stress and temperature for the demagnetization of the magnetic recording disk induced by sliding contact is important in practical applications.

There are many published studies using numerical methods to analyze the contact stress and temperature at the head/disk interface. Kennedy [10] presented a finite element model of the thermal response of sliding bodies subjected to a constant heat source. Gong and Komvopoulos [11,12] developed a fully coupled finite element analysis for an elastic-plastic patterned surface in contact with an elastic-plastic sphere and for a semi-infinite elastic solid against a rigid rough surface. Bhushan [13] calculated the maximum transient temperature rises for the assumed head-thin-film-disk over the contact area, which is 110°C for a Mn-Zn ferrite slider. Sofuoglu and Ozer [14] presented the rigid rough surface of a magnetic head and smooth surface of an elastic-plastic hard disk with a comprehensive thermoelastic-plastic contact analysis at the head/disk interface to study the stress and friction heating in the contact zone. The studies mentioned above provide useful knowledge about the thermomechanical analysis of a semi-infinite body in sliding contact. Mechanical energy is transformed into heat that results from friction under sliding contact. As frictional heat flows into the magnetic disk, the temperature at the contact interface of the sliding bodies rises, causing the contact area and stress change due to thermal expansion. Thus, the mechanical and thermal stress fields must be determined simultaneously. The author has studied the demagnetization of the longitudinal magnetic recording disk with a textured surface in contact against a head, based upon the finite element simulation under considering the coupling of contact stress and temperature at the interface [15,16].

[1]Corresponding author.

Contributed by the Tribology Division of ASME for publication in the JOURNAL OF TRIBOLOGY. Manuscript received September 15, 2008; final manuscript received November 22, 2009; published online March 11, 2010. Assoc. Editor: Yeau-Ren Jeng.

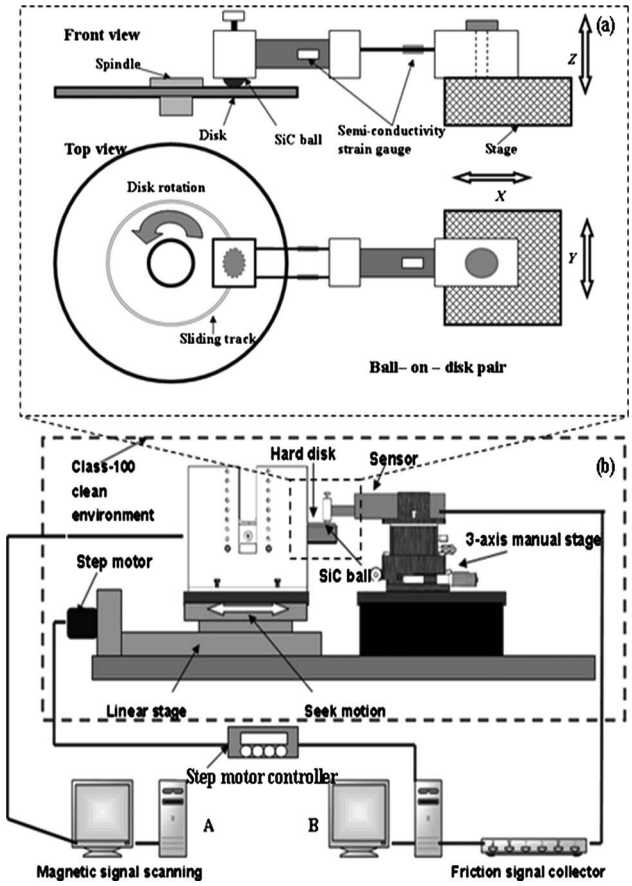

Fig. 1 Schematic sketch of ball-on-disk tribo-demagnetization designed apparatus: (*a*) magnetic disk scanning system and (*b*) ball-on-disk loading system

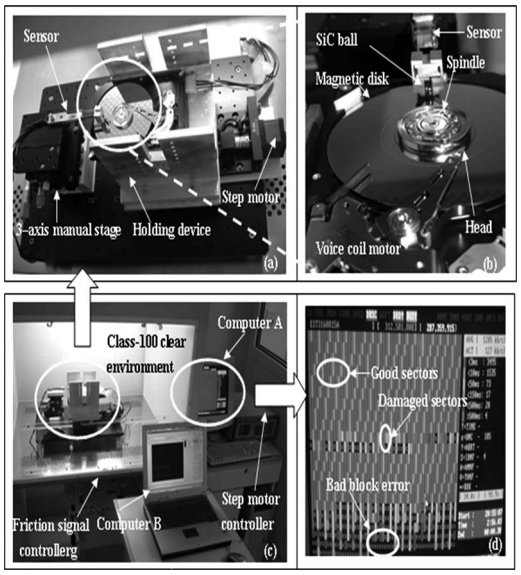

Fig. 2 Photos of tribo-demagnetization apparatus: (*a*) experiment rig, (*b*) ball-on-disk pair, (*c*) overview of the apparatus, and (*d*) screen capture of the scanning result

The purpose of this paper is to examine the critical conditions for the demagnetization of the perpendicular magnetic recording disk under sliding contact. For the purpose of such, a tribo-demagnetization test of perpendicular magnetic recording disk and the scan of the magnetic disk to evaluate the critical normal force and sliding velocity for the occurrence of demagnetization are carried out, and a thermomechanical coupling finite element model to calculate the critical stress and critical temperature for demagnetization of perpendicular magnetic recording disk is developed.

2 Experimental Method

2.1 Experimental Setup. Figure 1 shows the schematic sketch of a ball-on-disk tribo-demagnetization designed apparatus. The apparatus includes a ball-on-disk loading system and magnetic disk scanning system (shown in Fig. 1(*b*)).

The ball-on-disk loading system is used for the tribo-test. As is shown in Fig. 1(*a*), a SiC ball of 3.2 mm radius is fixed on the end of the force sensor, and normal force (W) is applied on the magnetic disk by moving the three-axis (X,Y,Z) manual stage, and normal force is also unloaded by releasing the screw of the stage. The sensor is made up of several metal beams, and the semiconductivity strain gauges stuck on the cantilever can measure the mini force (>0.05 mN) loaded on the disk. Figure 2(*a*) gives the photos of the tribo-demagnetization apparatus. The HDD is mounted on the linear stage by a clamp apparatus, as shown in Figs. 2(*a*) and 2(*b*), the design of the rig ensured the lever arm holding the SiC ball of sensor was initially and perfectly horizontal. The axle wire of the lever arm and the center of the HDD's spindle are in line, thus, the sliding velocity at the contact interface of disk is in the direction of tangent. The head of the HDD, which moves in the cross-track direction would affect the wear of the disk surface [17,18] and distort the track. In accordance with the work of the head of the HDD, we use the linear stage's reciprocating motion (arrow shown in the Fig. 1(*b*)), and the SiC ball is moved radially on the test disks to simulate the seek motion of the head of the HDD. The linear stage is driven by the step motor with a lead screw. Computer B will record the friction force and normal force, as well as control the linear stage (shown in Fig. 2(*c*)).

The magnetic disk scanning system is introduced to record the contact induced sectors in the tribo-test. The magnetic data of the hard disk are detected by head/disk system of the HDD, as shown in Fig. 2(*b*), and computer A records the damaged sectors by software MHDD 4.0 (shown in Fig. 2(*c*)). Figure 2(*d*) gives a screen cut of the scanning result of the magnetic disk after the tribo-test, and the different color blanks in the screen represent different scanning state of sectors. For example, white blanks indicate good sectors, red blanks mean damaged sectors, and x means usual bad block errors.

2.2 Experimental Conditions. The commercial 3.5 in. HDDs (Barracuda 7200.10 hard disk drive produced by Seagate in China) were used in the experiment. HDDs are based on perpendicular recording technology with a diameter of 95 mm Al-Mg substrate, and the capability of the hard disk drive is 160 Gb for single disks and the average areal recording density of the hard disk drive is 101 Gb/in.^{2}.

Figure 3(*a*) gives the static loading process of the sensor (HDD does not work), which indicates that the sensor can appropriately load the mini force on the disk. Figure 3(*b*) shows the changes of the normal force after starting the spindle of the disk. The normal force changes immediately after starting the HDD and keeps at a steady value until the spindle stops.

According to the average seek time (17 ms) of the HDD used in the experiment, a constant 34 μm displacement amplitude condition is considered, and the linear stage's reciprocating motion speed (stage moving speed) is 2 mm/s (17 ms $=34$ μm/2 mm/s). The SiC ball is moved radially on the test disks to simulate the seek motion of the real head in the hard disk drive. Other experimental conditions are listed in Table 1.

2.3 Test Procedure. Prior to the test, the SiC ball was cleaned

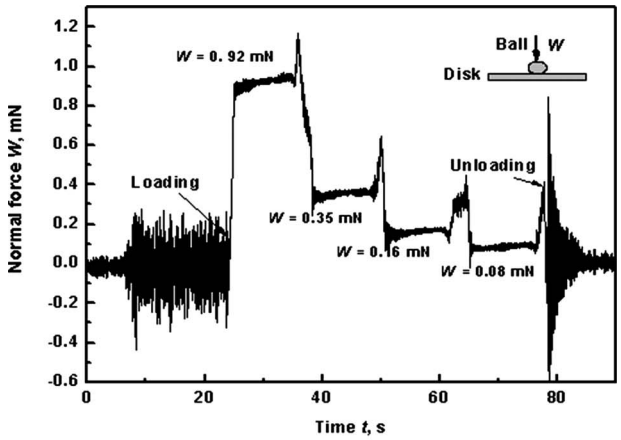

(a)

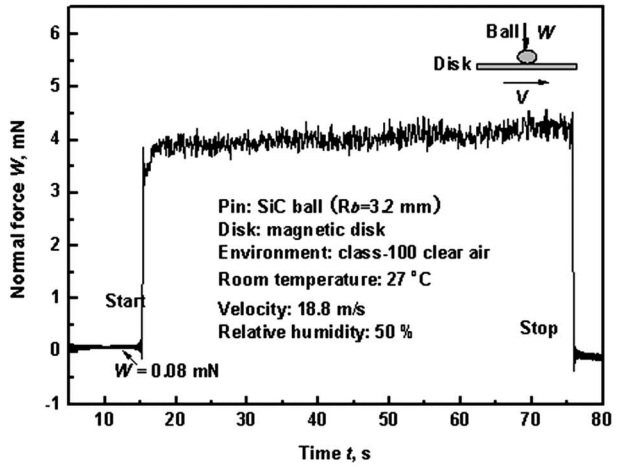

(b)

Fig. 3 (*a*) Static loading of sensor without the rotation of disk and (*b*) normal force with the rotation of disk

with acetone to remove all dusts from the surface. The test was performed at room temperature and with a constant relative humidity of 50%, under class-100 clean environment. The whole magnetic disk should be scanned before loading the normal force to make sure that there are no damaged sectors in the disk. The scanning time depends on the capability of the HDD; it costs 40 min to scan the whole disk before loading the normal force.

The HDD's cover was opened under class-100 clean environment. Then, the SiC ball was loaded on the loading position

Table 1 Experimental conditions of tribo-test

Conditions	Values
Normal force (mN)	0.085–1.185
Loading radius (mm)	23, 24, 25, 26, 27, 28, 29
Stage moving speed (mm/s)	2
Stage moving distance (μm)	34
Resolution of stage (μm)	0.625
Reciprocating times	10
Radius of SiC ball (mm)	3.2
Disk rotation speed (rpm)	7200
Areal recoding density (Gb/in.^{2})	101
Recording mode of magnetic recording disk	Perpendicular recording
Experimental environment	Class-100 clean environment

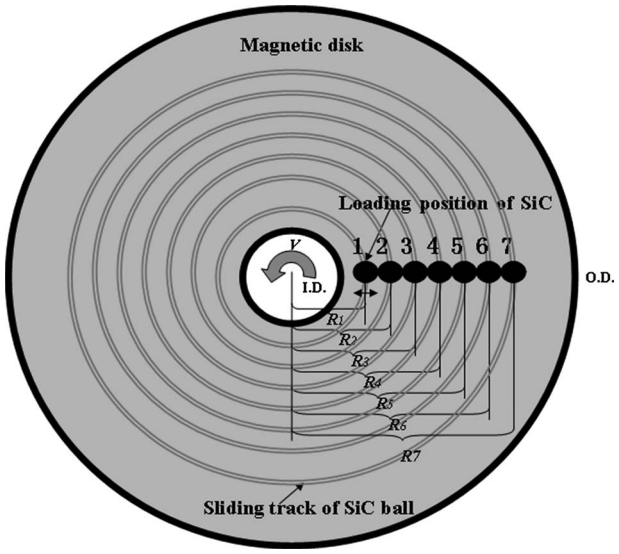

Fig. 4 Illustration of loading position of the tribo-demagnetization test

(shown in Fig. 4, R_1) with a mini force less than 2 mN, and the loading position was very close to the inner diameter (ID) at the beginning of test for better stability than the outer diameter(OD), as shown in Fig. 4. Seven loading positions on the disk surface ranging from 23 mm to 29 mm were tested in the experiment. The normal force and the friction force were recorded by the sensor with a sample of 200 Hz. The linear stage driven by the step motor made the HDD do a reciprocating motion to simulate the seek motion at a displacement of $S=34$ μm. After a total of 10 reciprocating times, the normal force W was unloaded by releasing the screw of the stage. The sectors in the contact areas of the magnetic disk were then scanned by the head with the software MHDD 4.0. The software was operated in DOS 7.0, and the contact induced damaged sectors were recorded in floppy disks. New tests (R_2, R_3, R_4, R_5, R_6, and R_7, as shown in Fig. 4) ran with different sliding speeds and different normal forces was then carried out.

3 Experimental Results

We define here that the demagnetization occurred only if the erased sectors in the tribo-test are more than one sector, based on the areal recording density of the HDD used in the experiment. Because the mean contact width ($2a$) of the ball-on-disk is 5 μm under the loads used in the experiment, the Hertzian contact area (A_a) of SiC ball is about 19.63 μm^2, and the real contact area (A_r) is 1.96 μm^2 ($A_r/A_a=0.1$ is used here, the detail calculating process of parameters mentioned above is given in Sec. 4.1). According to the average areal recording density of the magnetic disk used in the experiment, the area of the single recording sector was calculated, which is 3.04 μm^2 (the average areal recording density is 101 Gb/in.^{2}=0.15675 Gb/mm^2; the number of bytes/mm^2=$0.15675\times1024\times1024\times1024=1.68\times10^8$ bytes; the average area of a single byte=$1/(1.68\times10^8\times10^{-6})=5.95\times10^{-3}$ μm^2; so the area of a single recording sector=$512\times5.95\times10^{-3}=3.04$ μm^2). There are about 0.64 sectors (1.96 μm^2/3.04 μm^2=0.64) within the surface area of the magnetic disk in contact with the SiC ball. Thus, the demagnetization resulting from sliding contact happens if the erased sectors are more than one sector. The definition of the demagnetization of the magnetic disk relates with the contact width of the SiC ball and the initial areal recording density of the disk.

Figure 5 gives the critical curve in relation to normal force W and sliding velocity V for the demagnetization of the perpendicu-

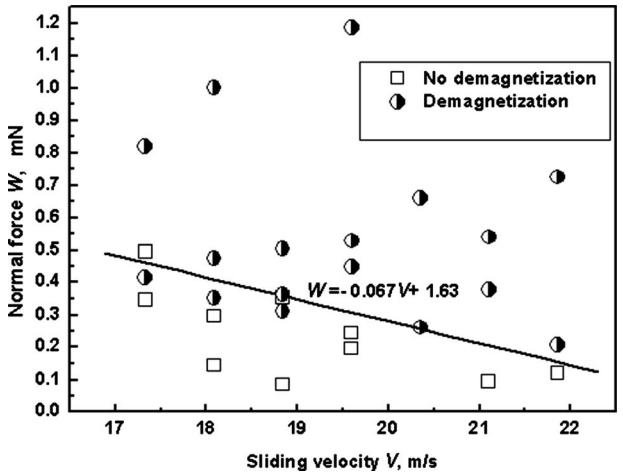

Fig. 5 Normal force versus sliding velocity and their effect on demagnetization of perpendicular magnetic recording disk (areal recording density is 101 Gb/in.^{2})

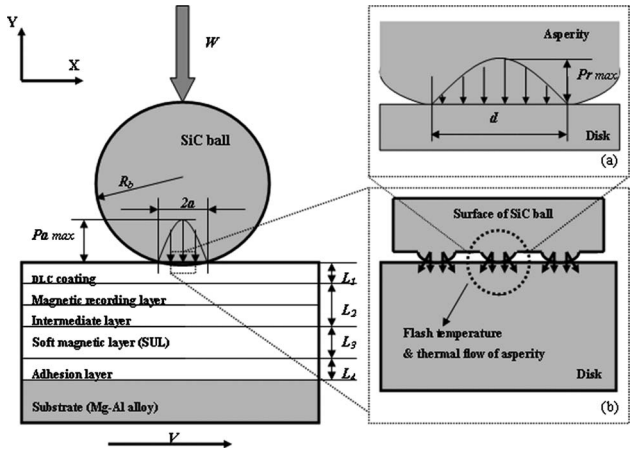

Fig. 6 Ball-on-disk contact model. (*a*) Equivalent roughness with multi-asperities of ball/disk and (*b*) single asperity contact.

lar magnetic recording disk used in the experiment. There are about 36 sectors erased by the ball-on-disk sliding contact with the normal force $W=0.819$ mN and sliding velocity $V=17.34$ m/s (loading position of SiC ball $R=23$ mm). Increasing the radius of the loading position, there are about 87 sectors erased with the normal force $W=0.379$ mN and sliding velocity $V=21.1$ m/s (loading position of SiC ball $R=28$ mm). Therefore, it can be concluded that the demagnetization normal force of the magnetic disk decreases with the increasing of velocity in the contact zone.

The whole area is divided into the nondemagnetization zone and demagnetization zone by the critical curve. All experiment data of the tribo-test are summarized in Fig. 5. The demagnetization of magnetic disks due to sliding contact when the normal force loaded on the disk is above the curve. The equation of the critical curve fitted is given as follows:

$$W = -0.067V + 1.63 \quad (17.3 \leq V \leq 21.9) \tag{1}$$

where W=the normal force loaded on the SiC ball (mN) and V=the sliding velocity of the SiC ball (m/s).

It should be noted that the range of the velocity limited by the constant spindle speed of the HDD and the erased sectors resulted from sliding velocity, as well as normal force. From the critical curve fitted by the tribo-demagnetization experimental results, the critical load of demagnetization for the perpendicular magnetic recording disk descends with the increasing of the sliding velocity.

4 Finite Element Analysis

Since the critical normal force and sliding velocity for the demagnetization of the hard disk were measured, the critical temperature and stress for the demagnetization of the perpendicular magnetic recording disk can be calculated by finite element analysis, based upon the measured critical curve. A ball-on-disk contact model is introduced to calculate the contact width under the critical normal force.

4.1 Contact Modeling. A ball-on-disk contact model combined with equivalent roughness was used to calculate the contact parameters for the development of the finite element model. Figure 6 shows the sliding contact geometry between the SiC ball and magnetic disk under normal force W, maximum contact pressure $(P_a)_{\max}$, and contact width $2a$. The magnetic recording layer and intermediate layer were combined to make a layer in the simulation. The effective elastic modulus of the coating surface related with the coating thickness [19], thus, the elastic modulus E_d of the magnetic disk, including the thicknesses of function layers in the perpendicular magnetic recording disk, was used to calculate the contact width. There are many asperities at the contact interface between the SiC ball and magnetic disk. In order to calculate the flash temperature of the asperity in the contact interface, as shown in Fig. 6(*b*), the roughness parameters of the SiC and magnetic disk surface to make asperities contact between the rigid SiC ball and a flat plane were combined. The combined surface roughness parameters are as follows [20]: standard deviation of surface heights $\sigma=0.654$ nm, mean radius of the curvature of asperity $r=6.384$ μm, and areal density of asperities $\eta=9.871$ μm^{-2}. Finally, the contact model, as shown in Fig. 6(*a*), was made between an asperity (d is the contact width of asperity) of the SiC ball and smooth flat disk surfaces to calculate the critical conditions. Whether contact is elastic or plastic, it is dependent on the plasticity index ψ [21]

$$\psi = \frac{E'}{H}\sqrt{\frac{\sigma}{r}}$$

$$\Psi < 0.6 \quad \text{elastic contact}$$

$$\Psi > 1.0 \quad \text{plastic contact} \tag{2}$$

where

$$E' = \frac{1}{\left[\dfrac{(1-\upsilon_d^2)}{E_d} + \dfrac{(1-\upsilon_b^2)}{E_b}\right]} \tag{3}$$

where E'=composite Young's modulus; E_b=Young's modulus of SiC ball, $E_b=450$ GPa [6]; E_d=Young's modulus of the magnetic disk, $E_d=100$ GPa [20]; υ_b=the Poisson's ratio of the SiC ball; υ_d=the Poisson's ratio of the magnetic disk, $\upsilon_b=\upsilon_d=0.3$; then, E' is obtained, $E'=89.9$ GPa; H=hardness of the softer material, $H=H_d=7.9$ GPa; σ=standard deviation of the surface asperities' heights; r=mean radius of the curvature of asperity, and η=areal density of asperities. Inserting Eq. (3) into Eq. (2), and ψ is obtained, $\psi=0.16$, the contact between the SiC ball and disk is elastic.

As the contact between the SiC ball and magnetic disk is elastic, the contact half-width (a), Hertzian contact area (A_a), and mean pressure of contact zone (P_a), calculated based Hertzian contact theory [21], are

$$a = \left(\frac{3WR_b}{4E'}\right)^{1/3} \tag{4}$$

$$A_a = \pi a^2 \tag{5}$$

$$P_a = \frac{W}{\pi a^2} \tag{6}$$

where W=the normal force applied on the SiC ball, W =0.47 mN; R_b=the radius of the SiC ball, R_b=3.20 mm; then, the contact half-width is calculated, a=2.32 μm. Inserting Eq. (4) into Eqs. (5) and (6), A_a and P_a are obtained as A_a=16.92 $\times 10^{-2}$ m^2 and P_a=27.67 MPa.

The ratio of the real contact area and Hertzian contact area (A_r/A_a) is given as [22]

$$\frac{A_r}{A_a} = \frac{3.2P_a}{E'\sqrt{\frac{\sigma}{r}}} \tag{7}$$

where σ=0.654 nm and r=6.384 μm; A_r/A_a is obtained, A_r/A_a =0.1.

The area-weighed-average diameter (d) and the mean real pressure (P_r) of asperity in the contact zone are as follows [22]:

$$d = 2\sqrt{\frac{3A_r}{\eta\pi A_a}} \tag{8}$$

$$P_r = \frac{W}{A_r} \tag{9}$$

Inserting Eq. (5) into Eq. (7), A_r is obtained, A_r=1.65 $\times 10^{-12}$ m^2; η=9.871 μm^{-2}. From Eqs. (8) and (9), d and P_r are calculated, d=194 nm; P_r=284.3 MPa.

The steady state time t_s is defined and taken as the time for the temperature to reach 90% of the steady state values [23]

$$t_s = \frac{3d^2}{4\kappa_{eq}}\left(\frac{2\kappa_{eq}}{Vd}\right)^{7/6} \tag{10}$$

where [24]

$$\kappa_{eq} = l/(l_1/\kappa_1 + l_2/\kappa_2 + l_3/\kappa_3 + l_4/\kappa_4) \tag{11}$$

$$\kappa = k/\rho c \tag{12}$$

where k_{eq}=the equivalent thermal diffusivity, κ_{eq}=3.05 $\times 10^{-6}$ m^2/s; l_1=thickness of the DLC layer, l_1=2$\times 10^{-9}$ m; l_2 =thickness of the magnetic recording layer and intermediate layer, l_2=35$\times 10^{-9}$ m; l_3=thickness of $Ni_{81}Fe_{19}$ layer, l_3=80 $\times 10^{-9}$ m; l_4=thickness of the NiP layer, l_4=10$\times 10^{-9}$ m; κ_1 =thermal diffusivity of the DLC layer, κ_1=0.62$\times 10^{-6}$ m^2/s; κ_2 =thermal diffusivity of the CoCrPt layer, κ_2=1.40$\times 10^{-6}$ m^2/s; κ_3=thermal diffusivity of $Ni_{81}Fe_{19}$ layer, κ_3=8.64$\times 10^{-6}$ m^2/s; and κ_4=thermal diffusivity of the NiP layer, κ_4=2.40 $\times 10^{-6}$ m^2/s; Inserting Eqs. (11) and (12) into Eq. (10), t_s is calculated as t_s=0.019 μs.

Finally, one of the finite element model parameters under critical normal force W=0.47 mN and critical velocity V =17.34 m/s was obtained: d=contact diameter of asperity, d =194 nm; t=0.03 μs ($t > t_s$); s=sliding distance of asperity, s =0.520 μm.

Eight critical normal forces and sliding velocities from the critical conditions curve (shown in Fig. 5) listed in Table 2 were selected to calculate the critical conditions for the tribo-demagnetization of the perpendicular magnetic recording disk under sliding contact. The contact width ($2a$) of the SiC ball ranged from $2a_{min}$=2.90 μm to $2a_{max}$=4.64 μm, and the contact diameter of asperity (d) ranged from d_{min}=153 nm to d_{max}=194 nm.

4.2 Finite Element Modeling. A commercial code (ANSYS 7.1) was used to define the finite element model, as well as to calculate the critical stress and temperature for the demagnetization of the magnetic disk. The finite element model simulated the effect of hard asperity (SiC ball) loaded against a softer surface (magnetic disk) under sliding contact.

Table 2 Contact width of SiC ball ($2a$) and contact diameter of asperity (d) under different critical conditions

Critical velocity V(m/s)	Critical normal force W(mN)	Contact width of SiC ball $2a$(μm)	Contact diameter of asperities d(nm)
17.34	0.47	4.64	194
18.10	0.42	4.46	190
18.84	0.37	4.27	186
19.60	0.32	4.07	182
20.36	0.26	3.84	176
21.11	0.22	3.58	170
21.86	0.16	3.27	163
22.62	0.11	2.90	153

Analysis was conducted under the plane strain condition. The lower surface (magnetic disk) was assumed to be a 2D, elastic, isotropic, and semi-infinite half-space. Default contact stiffness of the contact interface was applied in the finite element model. Geometric nonlinearity was included in the analysis by using the nonlinear geometry (NLGEOM) option. The automatic increment option in each step was used. As shown in Fig. 7, the finite element model of the magnetic disk size was 900 nm long by 130 nm thick to represent the semi-infinite body with 10 nm thick DLC layer, 35 nm thick CoPtCr layer, 80 nm thick $Ni_{81}Fe_{19}$ soft magnetic underlayer, and 10 nm thick NiP layer. The mesh was composed of a 2D four-nodded coupled area element (PLANE 13), two-node surface contact element. CONTACT 171 was used to represent contact and sliding between the 2D target surface and a deformable surface for thermomechanical analysis. Contact occurs when the element surface penetrates one of the target segment elements on a specified target surface. The target surface was defined by TARGET 169 to represent the 2D surface for the associated contact elements (CONTACT 171). The minimum size of quadratic elements was about 2 nm long by 1 nm deep. Sliding was taken along the positive x direction. The asperity was displaced laterally to a maximum sliding distance, while maintaining the interference distance constant. Table 3 shows the detailed physical and material properties of the finite element model.

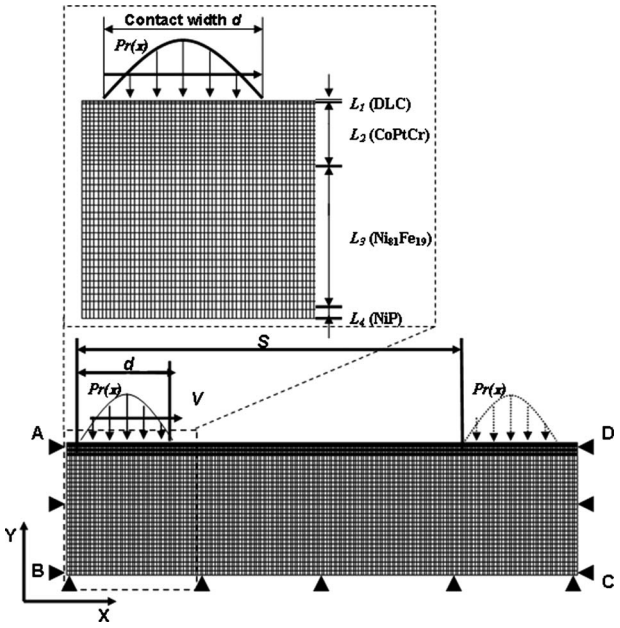

Fig. 7 Illustration of finite element model

Table 3 Material property of the ball and disk used in the finite element analysis

Property	Magnetic disk				Ball
	L_1 DLC	L_2 CoPtCr[b]	L_3 $Ni_{81}Fe_{19}$ [c]	L_4 NiP	SiC[b]
Thickness L/nm	2[a]	35	80	10	–
Poisson's ratio ν	0.30	0.30	0.30	0.36[d]	0.30
Young's modulus E/GPa	180	210	207	110[d]	450
Thermal expansion coefficient $\beta/10^{-6}$ K^{-1}	6.95	12.50	12.20	15.00	8.00
Thermal conductivity k/W(m K)$^{-1}$	1.24	6.03	35.00	9.30	16.77
Specific heat c/J(kg K)$^{-1}$	950	340	470	490	660
Density $\rho/10^3$ kg m^{-3}	2.10	12.67	8.62[e]	7.90	4.22

[a]Thickness of DLC (see Ref. [25]).
[b]Property of CoPtCr (see Ref. [15]).
[c]Property of $Ni_{81}Fe_{19}$ (see Ref. [4]).
[d]Poisson's ratio of NiP (see Ref. [26]).
[e]Density of $Ni_{81}Fe_{19}$ (see Ref. [27]).

4.3 Boundary Conditions for Finite Element Model. For the boundary conditions, the displacement of elements in the x direction of the borderline (AB, CD, shown in Fig. 7), as well as the y direction of the borderline (BC, shown in Fig. 7) of the lower surface (magnetic disk) were fixed, and that the borderlines (AB, BC, CD, shown in Fig. 7) were thermally insulated.

Contact pressure $P_r(x)$ was applied on top of asperity and it was transferred to the node of the finite element model, where

$$P_r(x) = \frac{3}{2}\frac{W}{A_r}\sqrt{1-\frac{(x-0.107)^2}{(d/2)^2}} \tag{13}$$

where W=normal force of the SiC ball; A_r=real contact area; x =position along the contact width of asperity; and d=contact width of asperity.

The dynamic coefficient of friction was determined as the ratio of the measured friction force and normal force. The coefficient of friction was assumed to be constant and does not depend on the variety of the normal force and velocity in this paper. Figures 8 and 9 represent two examples for the normal force and friction force during sliding contact without seeking motion. Figures 8(a) and 9(a) show the normal force variation with the sliding time in different sliding velocities during ball-on-disk contact. Normal force was loaded on the SiC ball by the cantilever of the sensor before starting the HDD's spindle. The normal force rose abruptly from 4.46 mN to 6.71 mN, and 6.96 mN to 9.31 mN, respectively (shown in Fig. 8(a) and 9(a)), and kept a steady state value when the HDD's spindle motor was started. The simultaneous acquisition of the friction force, as shown in Fig. 8(b) and 9(b), rose from 0 mN to 1.38 mN, and 0 mN to 1.63 mN, respectively, at once. When the disk stopped spinning, both the normal force and friction force moved back down to zero. From Figs. 8(b) and 9(b), it can be seen that the friction force has an obvious fluctuation during the sliding contact. The scatter band in the figure is typical and mainly due to the vibration within the experimental setup, as well as noise in the measurement system. The average friction coefficients μ is 0.2 (shown in Fig. 8, μ=0.21, and shown in Fig. 9, μ=0.18) and a constant coefficient of friction μ=0.2 tested in the experiment was applied on the contact interfaces of the finite element model.

4.4 Finite Element Analysis Results. Figure 10 gives the contours of the temperature in the semi-infinite medium of the perpendicular magnetic recording disk under sliding contact. The position of contact center is (0.627, 0.130) between asperity and DLC coating, and the maximum temperature (T_{max}=89.15°C) is in the position of (0.612, 0.130), which is behind the contact center in the DLC coating surface. The dash line in Fig. 10 shows the position of the contact center. Because the material properties (thermal conductivity, thermal expansion coefficient, and specific heat) of layers are different, the inflexions of contours come up in the interface of layers (interface between CoPtCr layer and $Ni_{81}Fe_{19}$ soft magnetic underlayer). In other words, the higher thermal conductivity of the soft magnetic underlayer is good for the conduction of heat caused by friction, and the heat is transmitted to the substrate (Al-Mg alloy disk) to decrease the temperature in the magnetic recording layer (CoPtCr layer). Furthermore,

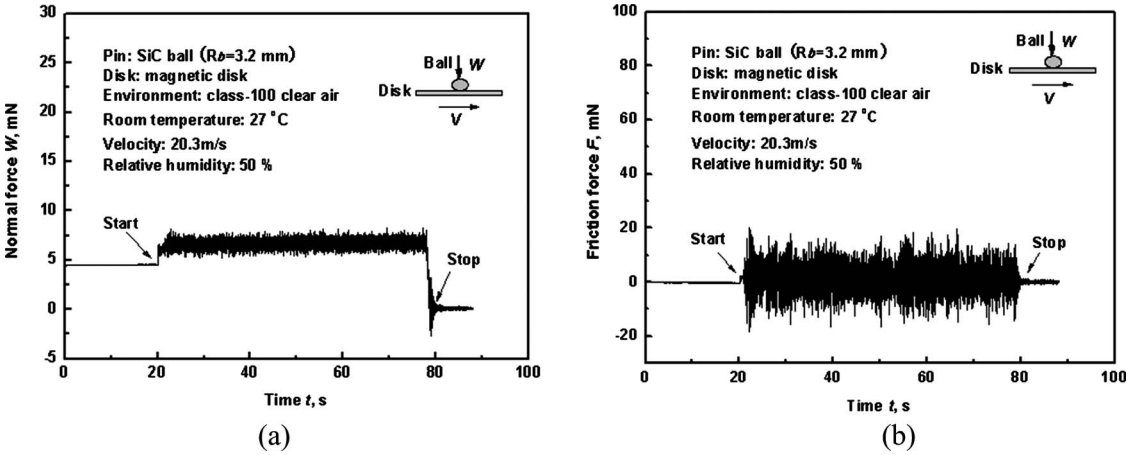

Fig. 8 (*a*) Normal force and (*b*) friction force during ball/disk contact, V=20.3 m/s

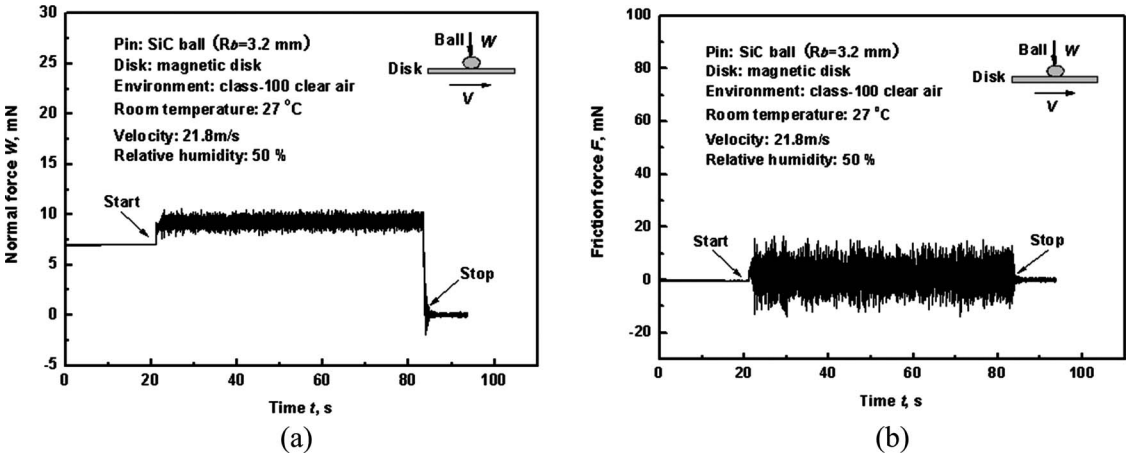

Fig. 9 (*a*) Normal force and (*b*) friction force during ball/disk contact, V=21.8 m/s

the DLC coating is about 2 nm thickness with the maximum temperature (T_{max}=89.15 °C) on the contact interface, but the maximum temperature in the magnetic recording layer, which is the interface between the DLC coating and CoPtCr layer, falls to 85.23 °C.

The demagnetization of the magnetic disk caused by stress could be explained by the inverse magnetostriction effect, which is that the magnetic intensity of magnetic domain will change with the dimension and volume induced by stress [28]. The easy axis orientation of the perpendicular magnetic recording disk is perpendicular to the track direction (the magnetizations lie perpendicular to the disk surface), so the x-component of stress (σ_x) will distort the dimension of the magnetic domain and affect the direction of magnetic intensity, so we take the x-component of stress σ_x to evaluate the critical stress for the demagnetization of the perpendicular magnetic recording disk. Figure 11(*a*) gives the contours of stress in the semi-infinite medium of the magnetic disk under sliding contact. The maximum x-component of stress ($(\sigma_x)_{max}$=−0.485 GPa) of the DLC coating and magnetic recording layer (CoPtCr layer) is in the position of (0.670, 0.125), as shown in Fig. 11(*a*), which is at the interface between the DLC coating and magnetic recording layer, and the position of the maximum stress is before the center of contact, while the position of the maximum temperature is behind the contact center. It means that the asperity pushes the subsurface material of the DLC coating and magnetic recording layer, which results in the compressive stress in the subsurface of the DLC coating close with the leading edge of asperity and tensile stress in the subsurface of the DLC coating close with the trailing edge of asperity. Figure 11(*b*) gives the contours of x-component of stress σ_x in the magnetic

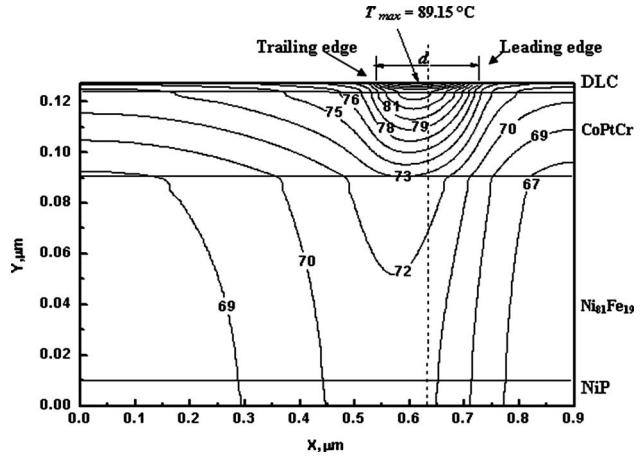

Fig. 10 Contours of temperature in the semi-infinite medium of magnetic disk under sliding contact (W=0.47 mN, S=0.52 μm, and V=17.34 m/s)

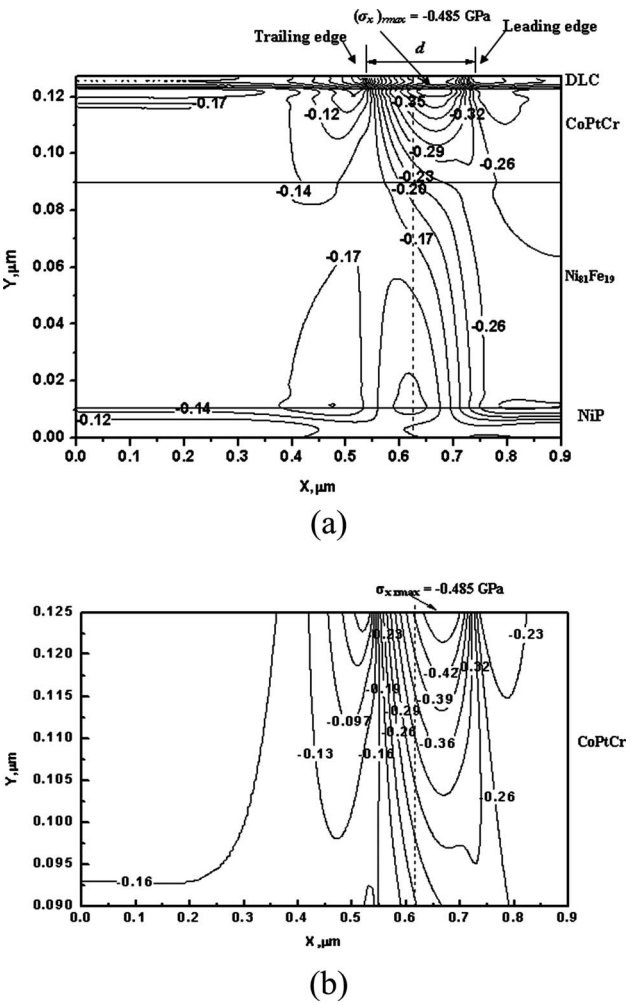

Fig. 11 (*a*) Contours of σ_x in the semi-infinite medium and (*b*) in the magnetic recording layer (CoPtCr) of magnetic disk under sliding contact (W=0.47 mN, S=0.52 μm, and V=17.34 m/s)

Table 4 FEA results of maximum temperature T_{max} and stress $(\sigma_x)_{max}$ in the magnetic recording layer (CoPtCr layer) under critical normal force W and critical sliding velocity V

Critical conditions		FEA results			
W (mN)	V (m/s)	$(T_{CoPtCr})_{max}$ (°C)	$(\bar{T}_{CoPtCr})_{max}$ (°C)	$(\sigma_x^{CoPtCr})_{max}$ (GPa)	$(\bar{\sigma}_x^{CoPtCr})_{max}$ (GPa)
0.47	17.34	85.23		−0.485	
0.42	18.10	87.36		−0.497	
0.37	18.84	89.47		−0.508	
0.32	19.60	91.63		−0.518	
0.26	20.36	93.96		−0.526	
0.22	21.11	95.51		−0.532	
0.16	21.86	97.18		−0.536	
0.11	22.62	98.86	$92.40(^{+6.46}_{-7.17})$	−0.537	$-0.517(^{+0.032}_{-0.020})$

recording layer (CoPtCr layer).

Table 4 gives other maximum temperature T_{max} and stress $(\sigma_x)_{max}$ in the magnetic recording layer (CoPtCr layer) under critical normal force W and sliding velocity V. Eight points were selected from the critical conditions curve as critical normal force and sliding velocity to calculate the critical conditions. The FEA results of maximum temperature $(T_{CoPtCr})_{max}$ in the magnetic recording layer ranged from 85.23°C to 98.86°C (the maximum temperature of the DLC coating $(T_{DLC}$ coating$)_{max}$ ranged from 89.15°C to 103.99°C), while the maximum stress $(\sigma_x^{CoPtCr})_{max}$ in the magnetic recording layer ranged from −0.485 GPa to −0.537 GPa. The critical temperature for demagnetization was defined here as the mean $(\bar{T}_{CoPtCr})_{max}$ of maximum temperature calculated with eight points of critical conditions. The critical compressive stress for demagnetization was also defined as the mean $(\bar{\sigma}_x^{CoPtCr})_{max}$ of the eight maximum stresses. Demagnetization occurs when the temperature in the magnetic recording layer exceeds T_d $\left(92.40(^{+6.46}_{-7.17})°\mathrm{C}\right)$, and the compressive stress exceeds σ_d $\left(-0.517(^{+0.032}_{-0.020})\ \mathrm{GPa}\right)$, which are responsible for the occurrence of demagnetization, thus, the demagnetization temperature and demagnetization compressive stress in the magnetic recording layer are

$$T_d = 92.40\begin{pmatrix}+6.46\\-7.17\end{pmatrix}°\mathrm{C} \tag{14}$$

$$\sigma_d = 0.517\begin{pmatrix}+0.032\\-0.020\end{pmatrix}\ \mathrm{GPa} \tag{15}$$

5 Discussion

In order to find the critical conditions, the present study considered the effect of stress and temperature on the tribo-demagnetization of the perpendicular magnetic recording disk. A tribo-demagnetization of the perpendicular magnetic recording disk using SiC ball-on-disk system, and the scan of the disk with the magnetic head, were carried out to evaluate the critical normal force and sliding velocity for the occurrence of demagnetization. Then the finite element model that considered the coupling of contact stress and temperature was used to calculate the critical conditions for the demagnetization of the perpendicular magnetic recording disk, based on the critical normal force and velocity curve tested in the tribo-demagnetization.

We consider that the demagnetization under sliding contact occurs only if the erased sectors are more than one in the contact zone. It means that the demagnetization definition depends on the contact width $(2a)$ of the SiC ball and the areal density of the magnetic disk. If the contact width was decreased to the track width of the magnetic recording disk in the experiment, the method can be also useful to invest the demagnetization of the single track of the magnetic disk. Additionally, the frictional vibration amplitude of the SiC ball that might be on the submicrometer-order in the down-track direction and cross-track direction could distort the disk tracks, as well as affect the demagnetization of the magnetic disk. The vibration amplitude would correlate with the normal force, and the very small normal force would provide hydrodynamic lubrication condition. Further study on this should be carried out in the near future.

The demagnetization temperature of magnetic materials depends on the Curie temperature, however, the demagnetization of magnetic disks due to sliding contact does not only relate with the Curie temperature of the material, but is also affected by the areal density of the magnetic disk, the coupling of temperature, and stress in the contact zone. Liu et al. [29] confirmed that severe erasure of data occurs even when the flash temperature is below the Curie temperature of the disk media. Li and Kumaran [30] measured the flash temperature during the intermittent head/disk contact using a magnetoresistive sensor in the range of 50–100°C with a disk spindle speed of 20 m/s (the contact width on the order of micrometer). In order to verify the critical temperature of the magnetic disk under sliding contact calculated by finite element analysis (FEA), the chromel-constantan thermal-couple sensor embedded in the polished pin against the magnetic disk was used to test the contact temperature during sliding contact, as shown in Fig. 12. A pin with a diameter of 0.25 mm was coved with asbestos to insulate the thermal conduction from the holder, and was fixed on the end of the force sensor. Normal force (W) was applied on the magnetic disk by moving the three-axis (X,Y,Z) manual stage, and it was also unloaded by releasing the screw of the stage. Temperature rise detected by the chromel-constantan thermal-couple sensor was displayed on the screen and was recorded. Various sliding velocity were tested to observe the contact temperature rise in the course of sliding contact. The pin was cleaned with acetone and all the tests were performed in the Class-100 clean environment with a constant relative humidity of 50%.

Figure 13 gives a typical change in temperature during sliding. The result showed that the temperature on the contact interface

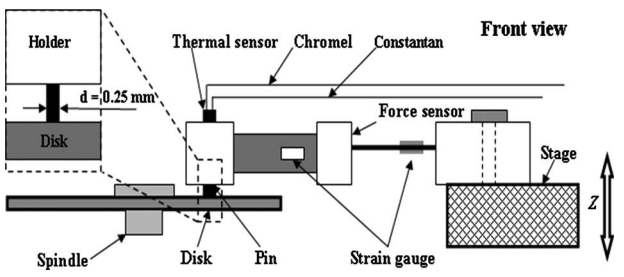

Fig. 12 Schematic sketch of pin-on-disk pair to test the sliding temperature

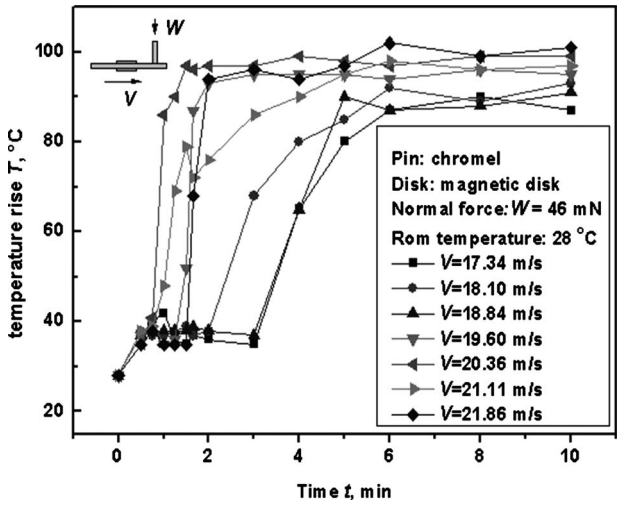

Fig. 13 Temperature rise versus time of magnetic disk under sliding contact

increased rapidly after the rotation of the disk and stayed at a relative steady state value (shown in Fig. 13). The minimum temperature of the steady state value was 87 °C (V=17.34 m/s), and the maximum temperature was 101 °C (V=21.86 m/s) during sliding. The temperature that rose at the contact interface relates with the normal force and sliding velocity. Though the temperature measured in the experiment was the bulk temperature of the pin, and the material property of pin (chromel) was different from SiC ball, the result may be helpful for understanding the finite element analysis results. Therefore, it is acceptable that the critical temperature calculated with the FEA is about 92.4 °C, based on the areal recording density of the hard disk drive used in the experiments.

6 Conclusions

The critical condition for the demagnetization of the perpendicular magnetic recording disk under sliding contact was studied. A demagnetization map for the perpendicular magnetic recording disk was proposed.

The following conclusions can be drawn from the present study.

1. A new method based on tribo-test and finite element model has been developed to calculate the critical stress and critical temperature of the magnetic recording disk.
2. The critical load of the demagnetization for the perpendicular magnetic recording disk descends with the increasing of sliding velocity, and the relationship between critical normal force W (mN) and sliding velocity V (m/s), is given by

$$W = -0.067V + 1.63 \quad (17.3 \leq V \leq 21.9)$$

3. The critical temperature T_d and compressive stress σ_d for the occurrence of the demagnetization of the perpendicular magnetic recording disk are given as

$$T_d = 92.40\begin{pmatrix} +6.46 \\ -7.17 \end{pmatrix} {}^\circ\mathrm{C}, \quad \sigma_d = 0.517\begin{pmatrix} +0.032 \\ -0.020 \end{pmatrix} \ \mathrm{GPa}$$

Acknowledgment

The authors would like to thank the National Nature Science Foundation of China under Grant No. 50775173, the National High-Tech Research and Develop Plan under Grant No. 2007AA04Z307, and Mechanical Engineering Research Laboratory of HITACHI for their support.

Nomenclature

W = normal force of SiC ball (mN)
V = sliding velocity of SiC ball (m/s)
R = loading position of SiC ball on magnetic disk (mm)
A_a = Hertzian contact area of SiC ball (m^2)
A_r = real contact area of SiC ball (m^2)
A_r/A_a = the ratio of real contact area and Hertzian contact area of SiC ball
σ = standard deviation of surface asperities heights (nm)
r = mean radius of curvature of asperity (μm)
η = areal density of asperities (μm^{-2})
ψ = plasticity index
H_d = hardness of magnetic disk (GPa)
v_b, v_d = Poisson's ratio of SiC ball and magnetic disk respectively
E_b, E_d = Young's modulus of SiC ball and magnetic disk respectively (GPa)
a = contact half-width (μm)
P_a = mean pressure of SiC ball in contact zone (GPa)
R_b = radius of SiC ball (mm)
d = contact width of asperity (nm)
P_r = mean real pressure of asperity in contact zone (GPa)
κ = thermal diffusivity (m^2/s)
κ_{eq} = the equivalent thermal diffusivity (m^2/s)
t_s = sliding time (μs)
k = thermal conductivity ($W(m\ K)^{-1}$)
c = specific heat ($J(kg\ K)^{-1}$)
β = thermal expansion coefficient (K^{-1})
ρ = density ($kg\ m^{-3}$)
T_{max} = maximum temperature (°C)
$(\sigma_x)_{max}$ = maximum x-component of stress (GPa)
T_d = critical temperature (°C)
σ_d = critical stress (GPa)

References

[1] Piramanayagam, S. N., 2007, "Perpendicular Recording Media for Hard Disk Drives," J. Appl. Phys., **102**, p. 011301.
[2] Khizroev, S., and Litvinov, D., 2004, "Perpendicular Magnetic Recording: Writing Process," J. Appl. Phys., **95**, pp. 4521–4537.
[3] Lee, K. M., Yeo, C. D., and Polycarpou, A. A., 2006, "Mechanical Property Measurements of Thin-Film Carbon Overcoat on Recording Media Towards 1 Tbit/in.^{2}," J. Appl. Phys., **99**(8), p. 08G906.
[4] Juang, J. Y., and Bogy, D. B., 2007, "Air-Bearing Effects on Actuated Thermal Pole-Tip Protrusion for Hard Disk Drives," ASME J. Tribol., **129**, pp. 570–578.
[5] Altshuler, K. J., Harrison, J. C., and Ackerman, E., 1999, "The Physical Effects of Intra-Drive Particulate Contamination on the Head-Disk Interface in Magnetic Hard Disk Drives," ASME J. Tribol., **121**, pp. 352–358.
[6] Fu, T. C., and Bogy, D. B., 1996, "Readback Signal Decrease Due to Dynamic Load Head-Disk Contacts," ASME J. Tribol., **118**, pp. 370–375.
[7] Suk, M., and Gillis, D., 1998, "Effect of Slider Burnish on Disk Damage During Dynamic Load/Unload," ASME J. Tribol., **120**, pp. 332–338.
[8] Suk, M., Dennig, P., and Gillis, D., 2000, "Magnetic Erasures Due to Impact Induced Interfacial Heating and Magnetostriction," ASME J. Tribol., **122**(1), pp. 264–268.
[9] Roy, M., and Brand, J. L., 2007, "Soft Particle-Induced Magnetic Erasure Without Physical Damage to the Media," ASME J. Tribol., **129**, pp. 729–734.
[10] Kennedy, F. E., 1984, "Thermal and Thermo Mechanical Effects in Dry Sliding," Wear, **100**, pp. 453–476.
[11] Gong, Z. Q., and Komvopoulos, K., 2004, "Mechanical and Thermo Mechanical Elastic-Plastic Contact Analysis of Layered Media With Patterned Surfaces," ASME J. Tribol., **126**, pp. 9–17.
[12] Gong, Z. Q., and Komvopoulos, K., 2005, "Thermo Mechanical Analysis of Semi-Infinite Solid in Sliding Contact With a Fractal Surface," ASME J. Tribol., **127**, pp. 331–342.
[13] Bhushan, B., 1992, "Magnetic Head-Media Interface Temperature Part–3 Application to Rigid Disks," ASME J. Tribol., **114**(3), pp. 420–430.
[14] Sofuoglu, H., and Ozer, A., 2008, "Thermomechanical Analysis of Elastoplastic Medium in Sliding Contact With Fractal Surface," Tribol. Int., **41**(8), pp.

783–796.
[15] Liu, J. Y., and Diao, D. F., 2006, "Demagnetization Map for Textured Magnetic Layered Disk in Contact Against Head," Surf. Coat. Technol., **201**(7), pp. 4273–4277.
[16] Liu, J. Y., and Diao, D. F., 2005, "Finite Element Analysis on Critical Conditions for Heat-Induced Demagnetization in Head/Disk Sliding Continuous Contact," Proceedings of the Third ASME World Tribology Congress, Washington, DC, pp. 687–688.
[17] Kawakubo, Y., Miyazawa, S., Nagata, K., and Kobatake, S., 2003, "Wear Life Prediction of Contact Recording Head," IEEE Trans. Magn., **39**(2), pp. 888–892.
[18] Kawakubo, Y., Ishii, M., and Sasaki, N., 2003, "Sliding-Pin Shapes and Lubricant Thickness Change on a Thin-Film Magnetic Disk," Tribol. Int., **36**(8), pp. 593–598.
[19] Diao, D. F., Kato, K., and Hokkirigawa, K., 1994, "Fracture Mechanisms of Ceramic Coatings in Indentation," ASME J. Tribol., **116**, pp. 860–869.
[20] Suh, A. Y., and Polycarpou, A. A., 2005, "Adhesive Contact Modeling for Sub-5-nm Ultralow Flying Magnetic Storage Head-Disk Interfaces Including Roughness Effects," J. Appl. Phys., **97**(10), p. 104328.
[21] Johnson, K. L., 1985, *Contact Mechanics*, Cambridge University Press, Cambridge, England, pp. 84–104.
[22] Bhushan, B., 1987, "Magnetic Head-Media Interface Temperature Part–1 Analysis," ASME J. Tribol., **109**(2), pp. 243–251.
[23] Leo, H. L., and Sinclair, G. B., 1998, "Flash Temperature Distributions at the Head-Disk Interface in Hard Disk Drives," ASME J. Tribol., **120**(3), pp. 536–541.
[24] Wang, J. W., Yuan, Z. M., Liu, B., and Ding, J., 2000, "Influence of Different Substrates on Potential Magnetic Degradation During Slider-Disk Impact," IEEE Trans. Magn., **36**(5), pp. 2686–2688.
[25] Menon, A. K., 2000, "Interface Tribology for 100 Gb/in.^{2}," Tribol. Int., **33**(5–6), pp. 299–308.
[26] Poon, C. Y., and Bhushan, B., 1996, "Nano-Asperity Contact Analysis and Surface Optimization for Magnetic Head Slider/Disk Contact," Wear, **202**(1), pp. 83–98.
[27] Holman, J. P., 1997, *Heat Transfer*, Mc Book Company, New York.
[28] Wan, D. F., and Ma, X. L., 1994, *Magnetic Physics*, University of Electronic Science and Technology Press, Chengdu, China, pp. 200–210.
[29] Liu, B., Man, Y. J., and Zhang, W., 2002, "Slider-Disk Interaction and Tribologically Induced Signal Decay," J. Magn. Magn. Mater., **239**(1–3), pp. 378–384.
[30] Li, Y., and Kumaran, A. R., 1993, "The Determination of Flash Temperature in Intermittent Magnetic Head/Disk Contacts Using Magnetoresistive Heads: Part II—Experimental Investigation," ASME J. Tribol., **115**(1), pp. 179–184.